To AIAA Inc.

NASA TECHNICAL MEMORANDUM

NASA TM X-52838

NASA TM X-52838

ESTIMATES OF FUEL CONTAINMENT IN A COAXIAL FLOW GAS-CORE NUCLEAR ROCKET

by Henry A. Putre
Lewis Research Center
Cleveland, Ohio

TECHNICAL PAPER proposed for presentation at
Sixteenth Annual Meeting of the American Nuclear Society
Los Angeles, California, June 28-July 2, 1970

ESTIMATES OF FUEL CONTAINMENT IN A COAXIAL FLOW GAS-CORE NUCLEAR ROCKET

by Henry A. Putre

Lewis Research Center
Cleveland, Ohio

TECHNICAL PAPER proposed for presentation at
Sixteenth Annual Meeting of the American Nuclear Society
Los Angeles, California, June 28-July 2, 1970

NATIONAL AERONAUTICS AND SPACE ADMINISTRATION

ESTIMATES OF FUEL CONTAINMENT IN A COAXIAL FLOW GAS-CORE NUCLEAR ROCKET

by Henry A. Putre

Lewis Research Center
National Aeronautics and Space Administration
Cleveland, Ohio

ABSTRACT

The main fluid mechanics problem in the rocket engine is that of predicting the contained fuel mass for various propellant-to-fuel flow ratios. The analysis described here calculates a dimensionless fuel mass, called the fuel volume fraction. This analysis uses a coaxial free-jet computer code, and eddy viscosity equations that had been developed for this code. The analysis also uses a smooth inlet velocity profile. The calculated variation of volume fraction with flow ratios, fuel radius, and fluid density is shown to be in general agreement with previous data.

SUMMARY

In the coaxial flow gas-core nuclear rocket concept the vaporized uranium fuel stream is surrounded by the lighter, faster moving hydrogen propellant stream. This coaxial flow provides fuel containment at the very high fuel temperatures. The fuel containment is limited by turbulent mixing due to the large velocity differences between the propellant and fuel streams. Therefore, the main fluid mechanics problem is that of predicting the contained fuel mass for various flow ratios. Such information is needed for criticality tests and for system optimization studies.

This paper describes a turbulent coaxial flow analysis that predicts fuel mass in the reactor cavity. This analysis uses an existing coaxial free-jet computer code, and an eddy viscosity equation previously evaluated from a free-jet data fit. For this study smooth inlet velocity profiles based on experimental data are specified as input in the computer code. The fuel volume fraction, defined as the fraction of the cavity volume oc-

E-5753

cupied by pure fuel, is used as a measure of the fuel mass. The fuel volume fraction is calculated for propellant-to-fuel flow ratios of 10 to 100, fuel-to propellant density ratios of 1.0 to 4.7 and fuel-to-cavity radius ratios of 0.5 to 0.7. The cavity length is fixed equal to the cavity diameter. These values are within the ranges of interest for a gas-core engine. The calculated volume fractions are compared with experimental data for this range of conditions.

The purpose of this study is to compare predicted fuel volume fractions, from an analysis based on free-jet experimental data, with experimental data from a second different and independent set of experiments on a cavity with side and end walls. In addition the calculated fuel volume fractions are compared with the desired engine design values, as determined by propulsion system requirements.

The calculated fuel volume fractions agree with most of the data to within ±30 percent. The analysis predicts the experimentally observed variation with density ratio and radius ratio. However, the predicted decrease of volume fraction with flow ratio is greater than shown by the data. The analysis and the data predict that the desired engine fuel volume fraction of 0.20 at the flow ratio of 50 can be obtained at a density ratio of 1.0 and a radius ratio near 0.7. This analysis also has resulted in a simple correlating equation for fuel volume fraction that is increasingly conservative as the propellant-to-fuel mass flow ratio increases above 50.

INTRODUCTION

The gas-core nuclear rocket is a proposed interplanetary propulsion system capable of high specific impulse (greater than 1500 sec) and high thrust (of the order of 500 000 lb). In the coaxial flow concept, shown in figure 1, the vaporized uranium fuel stream is surrounded by the lighter, faster moving, hydrogen propellant stream. The propellant stream is heated to about 10 000° R by thermal radiation from the fissioning fuel core which is at a temperature of about 100 000° R.

The coaxial flow provides the critical mass containment at the very high fuel temperatures without the solid-core engine fuel element material

problems. The penalty for this type of containment is that fuel is lost from the cavity due to turbulent mixing between the fuel and the propellant stream. According to Ragsdale (ref. 1) a desirable engine should contain enough fuel to give a fuel volume fraction of at least 20 percent at propellant-to-fuel mass flow ratios above 50. Reference 1 defines the fuel volume fraction as the fraction of the cavity volume occupied by pure fuel vapor if it were gathered into a central volume at its original temperature and cavity pressure.

The main fluid mechanics problem is that of predicting the fuel mass or fuel volume fraction for various propellant-to-fuel flow ratios and density ratios, and fuel-to-cavity radius ratios. Such information is needed for nuclear criticality studies, and for engine performance analyses, as for example in reference 2. This report presents the main features of an analysis for predicting fuel volume fraction.

The purpose of this report is to compare the predicted fuel volume fractions, from an analysis based on coaxial free-jet experimental data, with experimental data reported by Johnson (ref. 3) for coaxial flow in a cavity with side and end walls. In addition the calculated fuel volume fractions are compared with the desired engine design values from reference 1.

Most of the literature that applies to the engine flow has been experimental rather than theoretical. This is because turbulent analyses depend on turbulent property correlations, especially eddy viscosity, that are not reliable at the short cavity lengths and high velocity ratios in the engine. The present analysis incorporates most features of the flow and should help in interpreting the experimental data. Also it should prove useful in guiding future experiments on the coaxial cavity flow.

This analysis uses a turbulent coaxial flow computer code by Donovan and Todd (ref. 4) which solves the boundary layer equations for the isothermal two-fluid free jet. The eddy viscosity equations to be used are those evaluated by Putre (ref. 5) from Zawacki and Weinstein's (ref. 6) free-jet data. These eddy viscosity equations account for the different turbulent flow structure close to the inlet and far downstream. Reference 5 also concluded that a realistic inlet velocity profile must be specified in the computer code rather than a simple step profile. Thus the specified inlet velocity profiles for this study are based on inlet measurements by Johnson

(ref. 3). The cavity walls are defined in a way consistent with the free-jet code. The fuel containment is described in terms of dimensionless parameters, so that the predictions of fuel mass can be extended to the higher temperatures and pressures in the full-scale engines.

SYMBOLS

c	fuel mole fraction, concentration
L	cavity length
m	flow rate
R	specified radius
r	radial co-ordinate
$r_{1/2}$	velocity half radius, location where $u = 1/2(U_P + u_{\ell})$
Sc	Schmidt number
U	specified axial velocity
u	local axial velocity
VF	fuel volume fraction, defined as the fraction of the cavity occupied by pure fuel if it were gathered into a central volume
v	local radial velocity
x	axial coordinate
x_{12}	eddy viscosity cutoff location
y	fuel mass fraction
ϵ_1, ϵ_2	eddy viscosity (eqs. (4) and (5))
η	dimensionless flow ratio coordinate, eq. (8)
ρ	local density
φ	dimensionless volume fraction coordinate, eq. (9)

Subscripts:

B	buffer, used in describing the inlet velocity profile width

C cavity

F fuel, center stream

P propellant, outer stream

℄ centerline

ANALYSIS

In the coaxial flow concept a solid fuel rod is fed into the cavity and is vaporized by fission heating to form the fuel vapor cloud, as in figure 1. Downstream of plane A-A shown in figure 1, the fuel is assumed completely vaporized with the flow being nearly parallel. This downstream region will be analyzed here and was studied experimentally by Johnson (ref. 3).

Flow Model

The model analyzed is shown in figure 2. The model is basically an isothermal free jet, and use is made of the computer solution from Donovan and Todd (ref. 4). The side walls are included by assuming they coincide with the streamline that goes through $r = R_C$ at the inlet as shown in figure 2. The end wall is included as a porous wall at $x = 2R_C$. These walls are used for calculating the fuel volume fraction in the cavity.

The equations that are solved are the turbulent momentum and mass diffusion equations with the boundary layer assumptions and no pressure gradients. These are

The continuity equation:

$$\frac{\partial \rho u}{\partial x} + \frac{1}{r}\frac{\partial}{\partial r}(r\rho v) = 0 \tag{1}$$

The momentum equation:

$$\rho u \frac{\partial u}{\partial x} + \rho v \frac{\partial u}{\partial r} = \frac{1}{r}\frac{\partial}{\partial r}\left(r\rho\epsilon \frac{\partial u}{\partial r}\right) \tag{2}$$

The mass diffusion equation:

$$\rho u \frac{\partial y}{\partial x} + \rho v \frac{\partial y}{\partial r} = \frac{1}{r}\frac{\partial}{\partial r}\left(\frac{r\rho\epsilon}{Sc}\frac{\partial y}{\partial r}\right) \tag{3}$$

The initial and boundary conditions are

$$\left.\begin{array}{lll} u = f(r), & y = 1.; & 0 \le r \le R_F \\ u = f(r), & y = 0; & r > R_F \end{array}\right\} \text{ at } x = 0$$

$$\left.\begin{array}{llll} \dfrac{\partial u}{\partial r} = 0, & v = 0, & \dfrac{\partial y}{\partial r} = 0; & r = 0 \\ u \to U_P, & y \to 0; & r \to \infty & \end{array}\right\} \text{ at } x \ge 0$$

The analysis includes the following modifications in the computer code of reference 4: eddy viscosity formulation, inlet velocity profile, and volume fraction calculation.

Eddy Viscosity

The continuous two-region eddy viscosity which was evaluated in reference 5 is used in the code. This eddy viscosity variation was found to give the best data fit for the data of reference 6. The equations are:

for the region near the inlet

$$\epsilon_1 = 0.0015\, x(U_P - U_F) \qquad \text{for } x \le x_{12} \tag{4}$$

and downstream

$$\epsilon_2 = 0.034\, r_{1/2}(U_P - u_{\text{¢}}) \qquad \text{for } x > x_{12} \tag{5}$$

The location of x_{12} is defined in reference 5 to be where $\epsilon_1 = \epsilon_2$. In the present calculations the cavity is usually shorter than x_{12}, and ϵ_2 rarely applies. The Schmidt number in equation (3) is assumed to be $Sc = 0.7$.

Inlet Velocity Profiles

A smooth inlet velocity profile was achieved in reference 3 by using a porous material at plane A-A (see fig. 1). This smooth inlet velocity profile resulted in a larger fuel containment and less large scale fluctuations than had previously been observed with a discontinuous or step velocity profile. In addition the smooth inlet velocity profile is preferred since it is a more realistic end condition for the upstream fuel vaporizing region in the engine.

An inlet velocity profile was selected for the computer code that closely resembled the measured profile in reference 3 extrapolated to the inlet. The equation for the smooth inlet velocity profile is:

$$u = U_F \qquad \text{for } 0 \le r \le R_F \tag{6a}$$

$$u = U_F + \frac{U_P - U_F}{2(R_B - R_F)^2}(r - R_F)^2 \qquad \text{for } R_F < r \le R_B \tag{6b}$$

$$u = U_P - \frac{U_P - U_F}{2(R_B - R_F)^2}(r - 2R_B + R_F)^2 \qquad \text{for } R_B < r \le 2R_B - R_F \tag{6c}$$

$$u = U_P \qquad \text{for } r > 2R_B - R_F \tag{6d}$$

The specified inlet velocity profile is generalized for various fuel-to-cavity radius ratios by means of the inlet profile half-radius, R_B, which is taken equal to the upstream buffer radius of reference 3. The values of $R_B/R_F = 1.14$, 1.22, and 1.3 from reference 3 then correspond to the radius ratios $R_F/R_C = 0.7$, 0.6, and 0.5. A step inlet velocity profile is also used as a calculation sensitivity check.

Fuel Volume Fraction

The fuel mass in the cavity is calculated as a normalized quantity called the fuel volume fraction (VF). This quantity was first suggested by Ragsdale (ref. 1) for describing the containment effectiveness of various flows. The fuel volume fraction is defined as the fraction of the cavity volume occupied by pure fuel vapor if it were gathered into a central volume at its original temperature and cavity pressure. For this analysis the cavity volume is defined by planes A-A and B-B, and the streamline through $r = R_C$ at the inlet, as shown in figure 2. The fuel volume fraction is then calculated from

$$VF = \frac{\text{Fuel mass in cavity}}{\text{Pure fuel density} \times \text{Cavity volume}} \tag{7}$$

With a known pure fuel density (for a specified cavity pressure and average temperature), the fuel volume fraction is a direct measure of the fuel mass contained in a full-size heated engine.

RESULTS AND DISCUSSION

The results of the analysis, which uses a free-jet computer code end eddy viscosity equations based on free-jet data, are discussed and compared to Johnson's (ref. 3) data for flow in a cavity with side and end walls. The analysis uses a smooth inlet velocity profile that is typical of the cavity flow of reference 3. Reference 3 gives experimental volume fractions for air-air and Freon-air flows in a cavity shape similar to that downstream of plane A-A in figure 1. The data used here is for inlet "B" in reference 3, for which velocity profiles were measured.

Velocity Profiles

Preliminary computer runs were made with various specified inlet velocity profiles including a step profile, a linearly increasing profile and a parabolic (smooth) profile. The results of these preliminary runs were compared with the velocity profile data reported for one run in reference 3. The sensitivity of the calculations to various specified inlet velocity profiles was thus determined. The differences between calculated and measured velocity profiles were significiently larger with the step inlet profile than with the other profiles. For the final calculations the parabolic (eq. (6)) was used because it gave slightly better agreement with the velocity data near the inlet than a linear profile. The parabolic or smooth profile is shown along with the extreme case of the step profile in figure 3(a).

The results of calculations with the two velocity profiles of figure 3(a) are shown in figure 3(b). A simple comparison is made here with data by plotting the streamline passing through $r = R_F$ at the inlet. The calculations and data used values of $U_P/U_F = 35$ and $\rho_F/\mu_P = 1.0$. The corresponding flow ratio for the data and the smooth velocity profile is $m_P/m_F = 80$, and for the step profile it is $m_P/m_F = 105$. The step profile calculation predicts too much necking down of the streamline and too much fuel acceleration compared to the smooth profile calculation and the data. (Essentially the same results were obtained with the step profile

velocity ratio changed to $U_P/U_F = 27$ for a flow ratio of 80). Figure 3(b) thus shows the importance of the specified inlet velocity profile.

A more detailed plot of measured velocity profiles and those calculated with the smooth inlet profile (eq. (6)) is shown in figure 4. The width of the profiles show fair agreement. This agreement was not significantly improved by additional refinements of the specified inlet velocity profile (eq. (6)). The difference between the data and calculations near the side wall is partly the result of wall shear decelerating the flow. This wall shear was not included in the analysis. However, these velocity differences should not significantly affect the fuel volume fraction. They occur near the wall, where the fuel concentrations are small and therefore do not affect the fuel volume fraction very much. The discrepancy in the velocity profiles in the downstream centerline region (as indicated by the velocity profiles at $x/R_C = 1.2$ in fig. 4) may be significant in determining fuel volume fractions. In a mixing process between two coaxially flowing gases at different velocities there is a close relationship between velocity and concentration distributions. In addition, because fuel concentrations are largest near the centerline, these concentrations are the most important contributors to the fuel mass integration and to the fuel volume fraction. However, because the integration process de-emphasizes the importance of local concentration variation, the calculated fuel volume fractions are better than might be inferred by examination of the velocity profiles alone.

CONCENTRATION PROFILES

A typical calculated fuel concentration distribution is shown in figure 5. The fuel concentration (mole fraction) contours are plotted here for $m_P/m_F = 50$, $\rho_F/\rho_P = 1.0$, and $R_F/R_C = 0.5$. The cavity wall shapes from this calculation and from reference 3 are also shown in figure 5. The concentrations are seen to be largest near the centerline and decrease in the downstream direction. Figure 5 shows that the side walls are well outside the calculated main fuel region. Therefore, wall shear should have little effect on concentrations in the main fuel region.

In order to show how the fuel region is affected by density ratio and radius ratio, several 50 percent fuel concentration contours are shown in fig-

ure 6 for a fixed flow ratio of $m_P/m_F = 50$. This contour is representative of the other contours, as in figure 5, and gives a fair idea of the size of the fuel region.

The contours for $R_F/R_C = 0.5$ and various fuel densities are shown in figure 6(a). Here it is seen that, as the fuel density increases, the fuel region shortens considerably. This shortening is due to increased turbulent mixing as the propellant-to-fuel velocity ratio becomes larger for the same flow ratio. The effect of increasing the fuel density is a decrease in volume fraction from 0.140 to 0.074 as ρ_F/ρ_P goes from 1.0 to 4.7.

Similar contours for $\rho_F/\rho_P = 1.0$ and various fuel radii are shown in figure 6(b). The obvious effect of increasing the fuel radius R_F is to widen the fuel region at the inlet. The other less obvious effect is a shorter fuel region, due to increased turbulent mixing. The net effect of increasing the fuel radius is an increase in volume fraction from 0.140 to 0.195 as R_F/R_C goes from 0.5 to 0.7.

FUEL VOLUME FRACTION

The flow solutions were computed for various propellant-to-fuel flow ratios ranging from 10 to about 100. The computed fuel volume fractions are compared in figure 7 with the measured values from reference 3. The fuel volume fractions are computed for cavity shapes typically shown by the dashed lines in figure 5. Johnson gives in reference 3 measured fuel volume fractions for the cavity shape shown by the solid lines in figure 5. The aspect ratio for both cavities is fixed at $L = 2R_C$, which is typical for the gas-core rocket.

Figure 7(a) shows the volume fractions for the air-air and Freon-air density ratios at the radius ratio of $R_F/R_C = 0.5$. Figures 7(b) and (c) show similar results for the radius ratios of 0.6 and 0.7. The desired engine design (ref. 1) fuel volume fraction of 0.20 at a flow ratio of 50 is also shown in figures 7(a), (b), and (c).

Both the data and calculations show that, for the range of variables studied, the fuel volume fraction decreases with the propellant-to-fuel flow ratio, decreases with fuel density, and increases with fuel radius. The data and calculations are in closest agreement at the flow ratio of about 50.

All but four of the 23 data points in figures 7(a), (b), and (c) fall within ±30 percent of the calculated volume fractions.

The calculated trends with density ratio and radius ratio, shown in figure 7, are in general agreement with the data. However, the calculations predict a stronger decrease of volume fraction with increasing flow ratio than is shown by the data. The largest underestimates of volume fraction occur at flow ratios above about 100.

This discrepancy in the variation of volume fraction with flow ratio could probably be reduced by a more complicated computer solution that accounts for pressure gradients and for the actual cavity wall shape. In addition, since the eddy viscosity equations (eqs. (4) and (5)) strictly apply only for free-jet flow without side or end walls, further refinements in the eddy viscosity equations should reduce this discrepancy. However, until such improvements in computer solutions and eddy viscosity formulations are made, the present flow analysis gives increasingly conservative predictions of fuel volume fractions for fuel-to-propellant flow ratios greater than 50.

With regards to the design engine requirement, figure 7 shows that at the required flow ratio of 50 the computed volume fractions for the density ratio of 4.7 increase from 0.74 to 0.109 as radius ratio increases from 0.5 to 0.7. The corresponding volume fractions for a density ratio of 1.0 increase from 0.140 to 0.195. Thus the analysis predicts that the volume fraction of 0.20 for the design engine can be obtained at a density ratio of $\rho_F/\rho_P = 1.0$ and a radius ratio near $R_F/R_C = 0.7$. This result is in agreement with the data.

Correlating Curve

By cross-plotting the calculated results, it was possible to collapse the various volume fraction versus flow ratio curves in figure 7 into one correlating curve. This required that the calculated results be replotted in terms of the following grouped coordinates:

$$\varphi = (VF)\left(\frac{R_F}{R_C}\right)^{-2} \tag{8}$$

$$\eta = \left(\frac{m_P}{m_F}\right)\left(\frac{\rho_F}{\rho_P}\right)^{3/4}\left(\frac{R_F}{R_C}\right)^2 \tag{9}$$

The combination in φ was chosen because at low flow ratios the volume fraction must approach $(R_F/R_C)^2$. The combination in η is less obvious and was obtained by cross-plotting. The exponents in equation (8) are sufficient to correlate all the calculations in figure 7 to within ±5 percent of the curve shown in figure 8.

The data from reference 3 are also plotted in these new variables in figure 8. The data points are about evenly divided on either side of the curve. Eighty percent of the data points fall within ±30 percent of the correlating curve. For η greater than 10, which includes practical engine flows, the correlating curve can be written as:

$$\varphi = 1.95\,\eta^{-1/2} \tag{10}$$

or

$$VF = 1.95\left(\frac{m_P}{m_F}\right)^{-1/2}\left(\frac{\rho_F}{\rho_P}\right)^{-3/8}\left(\frac{R_F}{R_C}\right) \tag{11}$$

The data points show a different η dependence than equation (10). This is mainly because of the discrepancy in the flow ratio dependence noted in the above discussion on figure 7. However, it is important to note that fair agreement in figure 8 between the correlating curve from this analysis and the data has been obtained with a computer code and eddy viscosity equations that strictly apply only for a free jet, whereas the data is for a cavity with side and end walls. Although not obvious in figure 8 because of the coordinates used, the volume fractions predicted by equation (10) are in close agreement with the data at the propellant-to-fuel flow ratio of 50, and are increasingly conservative at flow ratios greater than 50.

CONCLUDING REMARKS

The fuel volume fraction in a coaxial flow gas-core nuclear rocket has been computed for various propellant-to-fuel mass flow ratios and density ratios, and various fuel-to-cavity radius ratios. The analysis uses a coaxial free-jet computer code from Donovan and Todd (ref. 4) and eddy viscosity equations derived from free-jet data (ref. 5). Preliminary calculations showed that a step inlet velocity profile in the code predicted too large flow accelerations. A smooth inlet velocity profile was finally specified in the computer code, and computed fuel volume fractions were compared with Johnson's (ref. 3) experimental data for a cavity with side and end walls.

The results of these calculations show that, for the ranges m_P/m_F = 10 to 100, ρ_F/ρ_P = 1.0 to 4.7, and R_F/R_C = 0.5 to 0.7, the analysis agrees with most of the experimental data to within ±30 percent. The analysis predicts the experimentally observed volume fraction variation with density ratio and with radius ratio. The predicted decrease of volume fraction with increasing flow ratio is stronger than that shown by the data. It should be noted that good general agreement between the calculations and data has been obtained with a computer code and eddy viscosity equations that strictly apply only for a free jet, but were used to analyze a cavity with side and end walls. This analysis predicts fuel volume fractions that are in close agreement with the data at the propellant-to-fuel flow ratio of 50, and are increasingly conservative at flow ratios greater than 50.

The algebraic correlating equation (eq. (11)) can be used in future parametric and system optimization studies. The analysis predicts, and the data confirm, that the desired engine design fuel volume fraction of 0.20 at a propellant-to-fuel flow ratio of 50 can be obtained a density ratio of 1.0 and a radius ratio of 0.7.

REFERENCES

1. R. G. RAGSDALE, "Are Gas-Core Nuclear Rockets Attainable?," AIAA Paper 68-570, (June 1968).

2. R. G. RAGSDALE, "Relationship Between Engine Parameters and the Fuel Mass Contained in an Open-Cycle Gas-Core Reactor," presented at the NASA-University of Florida Symposium on Research on Uranium Plasmas and Their Technological Applications, Gainesville, Fla., Jan. 7-9, 1970.

3. B. V. JOHNSON, "Exploratory Experimental Study of the Effects of Inlet Conditions on the Flow and Containment Characteristics of Coaxial Flows," United Aircraft Corp. Report H-910091-21, NASA CR-107051 (Sept. 1969).

4. L. F. DONOVAN and C. A. TODD, "Computer Program for Calculating Isothermal Turbulent Mixing of Two Gases," NASA TN D-4378 (1968).

5. H. A. PUTRE, "Improved Data Agreement Using New Eddy Viscosity Equations in a Coaxial Free-Jet Computer Code," NASA TN D-5835. (1970).

6. T. S. ZAWACKI and H. WEINSTEIN, "Experimental Investigation of Turbulence in the Mixing Region Between Coaxial Streams," NASA CR-959 (1968).

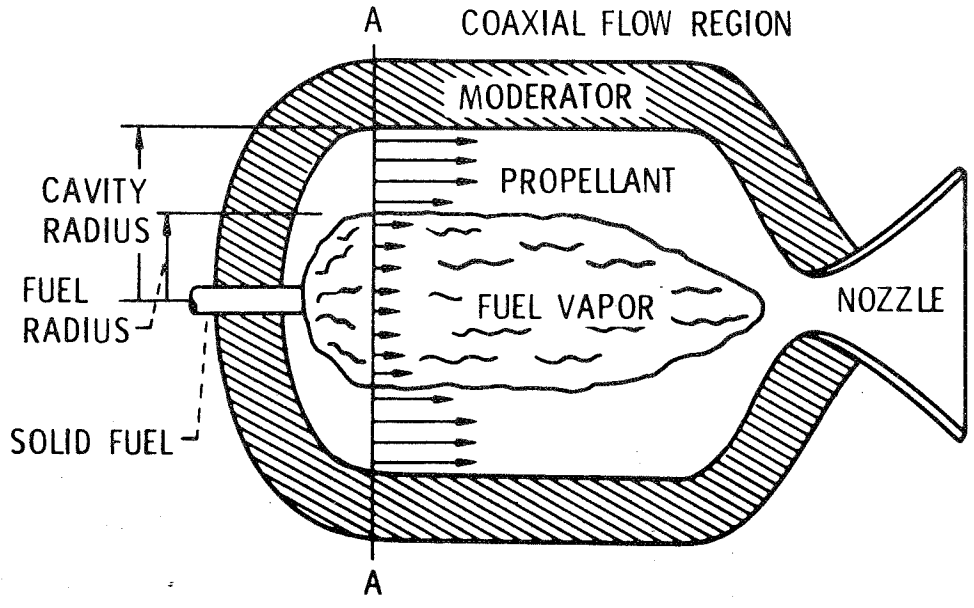

Figure 1. - Coaxial flow gas core nuclear rocket schematic.

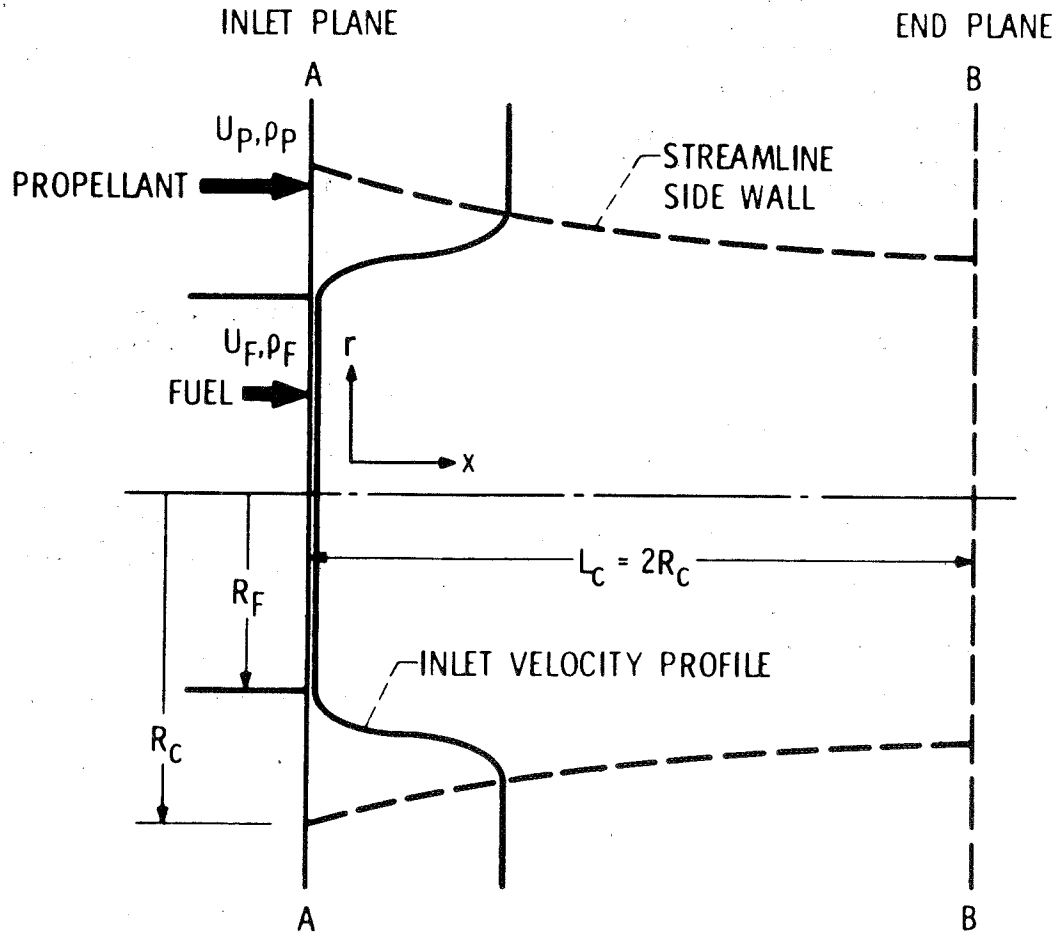

Figure 2. - Model of coaxial free-jet modified for gas core calculations showing typical inlet velocity profile, and cavity walls.

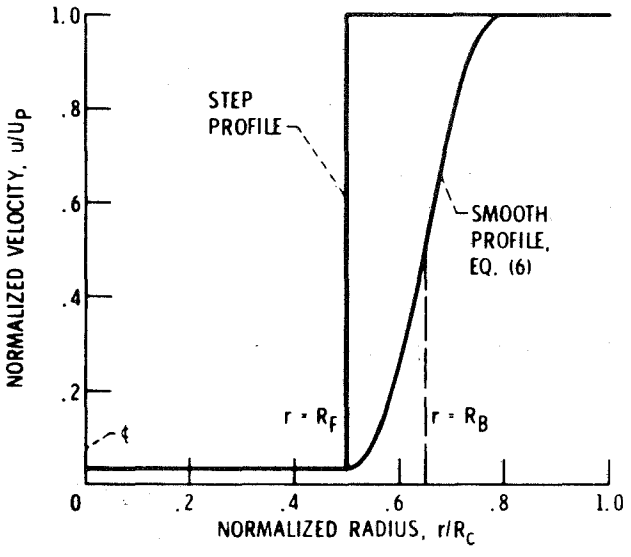

(a) Inlet velocity profiles.

Figure 3. - Streamlines from fuel inlet edge, for two inlet velocity profiles, compared to data (ref. 3). Velocity ratio U_P/U_F, 35; density ratio ρ_F/ρ_P, 1.0; radius ratio R_F/R_C, 0.5.

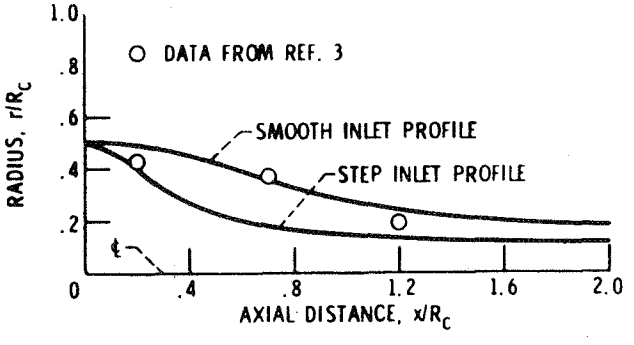

(b) Location of streamline from fuel inlet edge.

Figure 3. - Concluded.

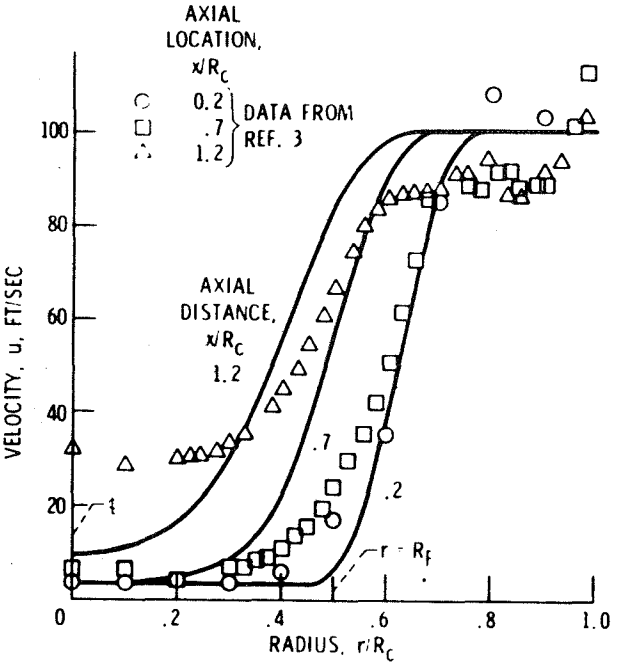

Figure 4. - Comparison of velocity profiles calculated with smooth inlet profile to data from ref. 3. Flow ratio m_P/m_F, 80; density ratio ρ_F/ρ_P, 1.0; radius ratio R_F/R_C, 0.5.

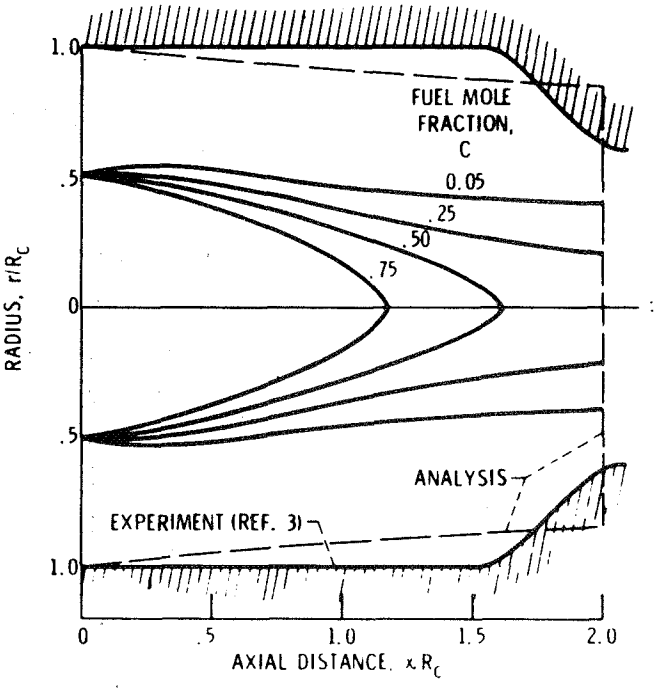

Figure 5. Location of fuel concentration contours and cavity walls from analysis compared to cavity walls from experiment. Flow ratio m_P/m_F, 50; density ratio ρ_F/ρ_P, 1.0; radius ratio R_F/R_C, 0.5.

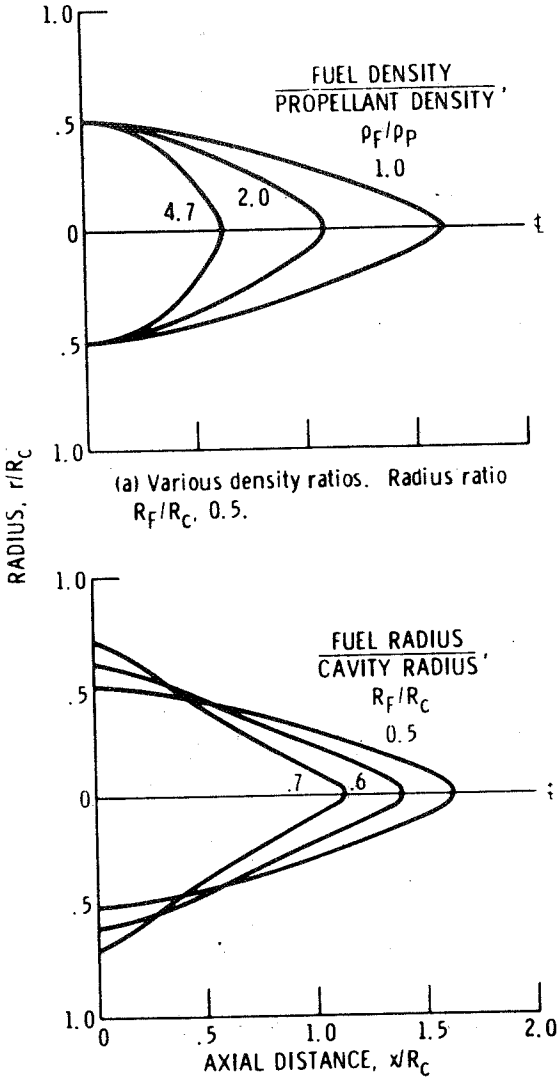

(a) Various density ratios. Radius ratio R_F/R_C, 0.5.

(b) Various radius ratios. Density ratio ρ_F/ρ_P, 1.0.

Figure 6. - 50 Percent concentration contours for various density ratios and radius ratios. Flow ratio m_P/m_F, 50.

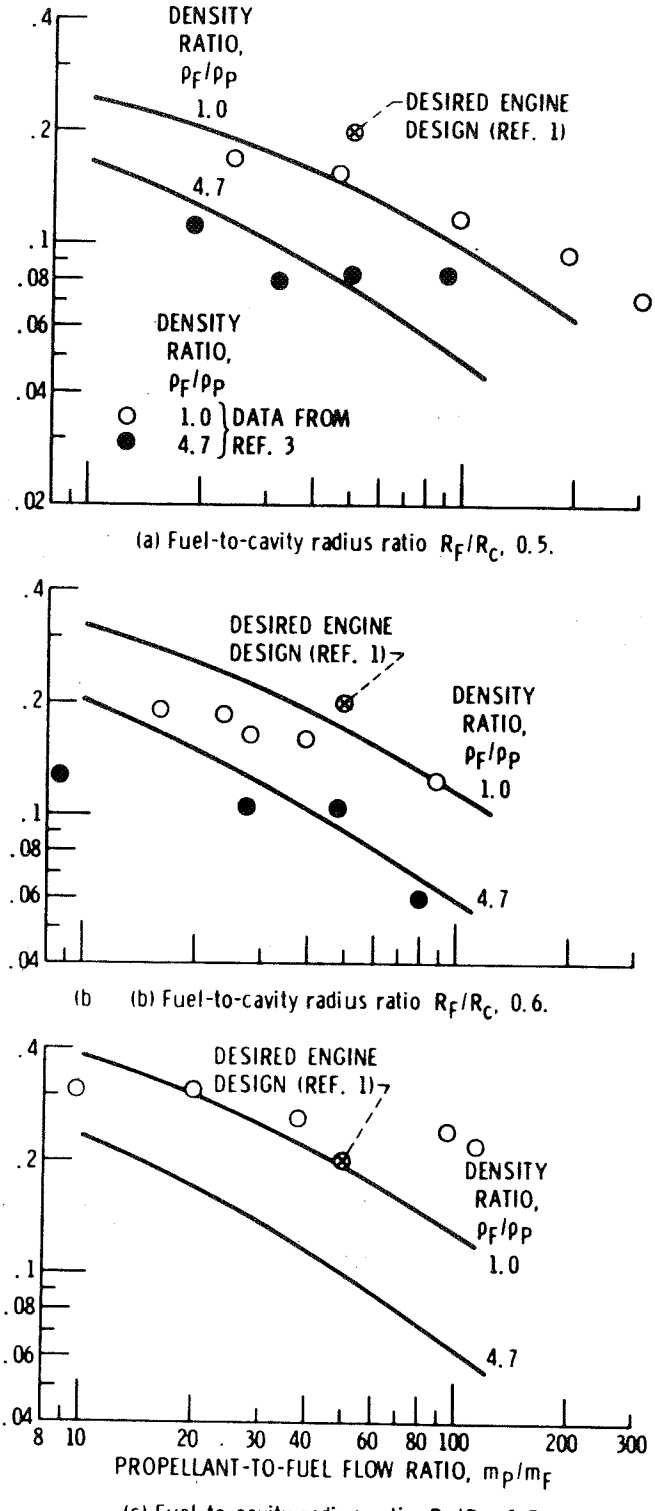

(a) Fuel-to-cavity radius ratio R_F/R_C, 0.5.

(b) Fuel-to-cavity radius ratio R_F/R_C, 0.6.

(c) Fuel-to-cavity radius ratio R_F/R_C, 0.7.

Figure 7. - Calculated variation of fuel volume fraction with flow ratio compared to data from ref. 3.

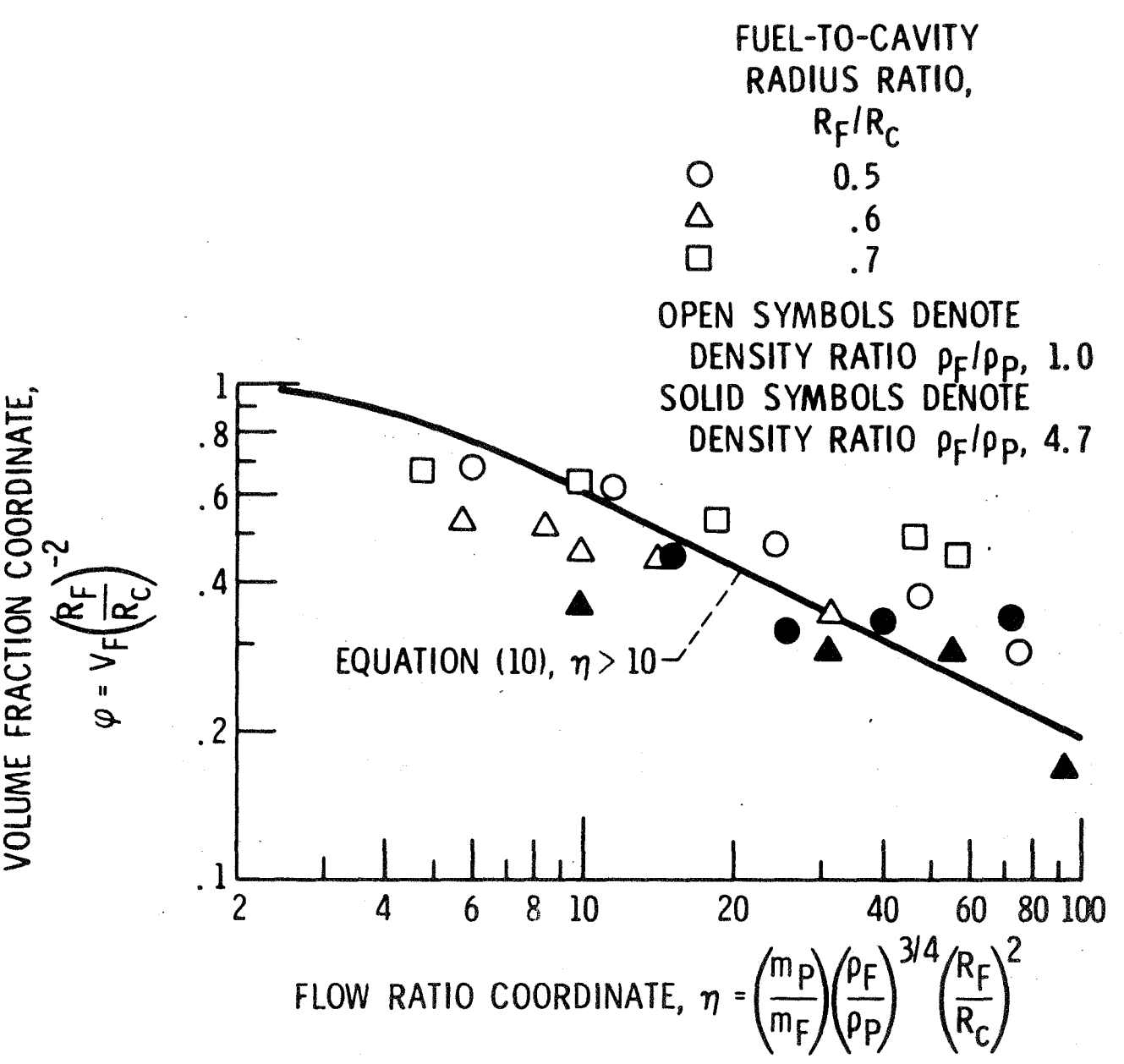

Figure 8. - Correlation curve compared with data from ref. 3.